-

COP9 signalosome component CSN-5 stabilizes PUF proteins FBF-1 and FBF-2 in *C. elegans* germline stem cells

Emily Osterli, Mary Ellenbecker, Xiaobo Wang[1], Mikaya Terzo, Ketch Jacobson, Ekaterina Voronina*

Division of Biological Sciences, University of Montana, Missoula, MT, 59812, USA

[1]current address: Southern Medical University, Guangzhou, China

*Corresponding author: ekaterina.voronina@umontana.edu

Keywords:

CSN-2, CSN-6, PUM1, CSN5, stem cells, oogenesis

Summary statement:

CSN-5 directly interacts with and stabilizes FBF-1/2 proteins, independently of CSN-5's function in the COP9 complex, thereby promoting stem cell maintenance and oogenesis in *C. elegans.*

Abstract:

RNA-binding proteins FBF-1 and FBF-2 (FBFs) are required for germline stem cell maintenance in *Caenorhabditis elegans* and regulate the dynamics of progenitor cell proliferation and differentiation. The mechanisms controlling FBF protein levels remain unknown. We identified an interaction between both FBFs and CSN-5, a component of the COP9 (constitutive photomorphogenesis 9) signalosome. Here, we find that the MPN (Mpr1/Pad1 N-terminal) metalloprotease domain of CSN-5 interacts with the PUF RNA-binding domain of FBFs and the interaction is conserved for human homologs hPUM1 and hCSN5. This interaction likely takes place outside of the COP9 holoenzyme. *csn-5* mutation results in destabilization of FBF proteins in germline stem cells leading to phenotypes consistent with a partial FBF loss of function. We propose that a COP9-independent role of CSN-5 in the PUF protein stability and function may be conserved across species, with implications for human stem cell biology and cancer.

Introduction:

Stem cells are a population of unspecialized cells with the capability to both self-renew and maintain the stem cell pool or to differentiate and support tissue maintenance (Morrison and Kimble, 2006). Stem cell function depends on faithful expression of essential developmental regulators (Morrison et al., 1997). A number of mechanisms controlling expression of stem cell machinery at the levels of epigenetics, transcription, and RNA stability have been widely studied (for examples, see Lee et al., 2016; Chen et al., 2020; Samuels et al., 2020; Demarco et al., 2022; Vogiatzoglou et al., 2022). However, mechanisms that maintain protein stability of stem cell regulators remain relatively unexplored.

We utilize the *Caenorhabditis elegans* germline to study stem cell regulators FBF-1 and FBF-2 (FBFs). The *C. elegans* gonad consists of two U-shaped arms, each with a population of stem and progenitor (SPC) cells at the distal end (Fig. 1A; Kimble and White, 1981). SPCs are maintained through the GLP-1/Notch signaling from the somatic niche cell (Austin and Kimble, 1987; Berry et al., 1997; Kimble and Crittenden, 2007). As the cells progress away from the niche, they begin to differentiate and enter meiosis before generating gametes at the proximal end (Hubbard, 2007; Pazdernik and Schedl, 2013; Voronina and Greenstein, 2016). The germlines produce sperm during larval development and switch to oogenesis in the young adults (Pazdernik and Schedl, 2013).

FBFs are RNA-binding proteins belonging to the highly conserved PUF (Pumilio and FBF) family (Wickens et al., 2002). FBFs are expressed in SPCs and act by binding to and repressing their target mRNAs (Zhang et al., 1997; Crittenden et al., 2002; Prasad et al., 2016). FBFs promote germline stem cell maintenance and *fbf-1 fbf-2* double mutant gonads lose their germline stem cells (Crittenden et al., 2002; Wickens et al., 2002; Wang and Voronina, 2020). Consistent with this function, many FBF targets encode developmental regulators, which are silenced in stem cells and then activated upon differentiation, such as the differentiation-promoting protein GLD-1 (Crittenden et al., 2002; Suh et al., 2009). FBFs also promote self-renewal of germline stem cells by repressing *cki-2* (Kalchhauser et al., 2011), a Cyclin E/Cdk2 inhibitor which regulates the decision to enter/exit the cell cycle (Buck et al., 2009). In addition to supporting stem cell proliferation, FBF-2 promotes stem cell differentiation and *fbf-2* mutant can form synthetic germline tumors due to delayed meiotic entry (Wang et al., 2020). The balance of FBF-1 and FBF-2 regulatory activities is important to determine the dynamics of proliferation and differentiation of *C. elegans* germline stem and progenitor cells (Wang et al., 2020). Additionally, FBF-1 and FBF-2 regulate sex determination by facilitating the switch from spermatogenesis to oogenesis (Zhang et al., 1997) as *fbf-1 fbf-2* double mutant gonads fail to undergo oogenesis, resulting in a masculinization of germline (Mog) phenotype where only sperm is produced (Crittenden et al., 2002). Despite these well-characterized functions of FBFs, the mechanisms regulating the levels of FBF proteins in stem cells remain unknown.

One prominent cellular mechanism impacting protein stability and steady-state levels involves the COP9 (constitutive photomorphogenesis 9) signalosome, a highly conserved enzymatic complex composed of eight subunits, denoted CSN1 to CSN8 (Qin et al., 2020). Although initially discovered for its role in regulation of transcription (Wei and Deng, 1992), the COP9 signalosome's best documented function is as a regulator of protein degradation (Wei et al., 1994; Chamovitz et al., 1996; Claret et al., 1996; Chamovitz, 2009). COP9 impacts protein degradation by removing a ubiquitin-like protein, NEDD8, from cullin subunits of E3 ubiquitin ligases (Cope et al., 2002; Lingaraju et al., 2014). This de-neddylation is essential to maintain the activity of cullin-based ubiquitin ligases and to facilitate the degradation of their substrates (Lyapina et al., 2001; Doronkin et al., 2003; Pintard et al., 2003; Wu et al., 2005). The overall architecture of COP9 resembles the 19S lid of the 26S proteasome, which is responsible for the majority of intracellular protein degradation (Enchev et al., 2012; Lingaraju et al., 2014). CSN subunits 1-4, 7, and 8 contain PCI (**P**roteasome, **C**OP9 signalosome, translation **I**nitiation factor) domains similar to the six subunits of the proteasome lid (Dessau et al., 2008; Hofmann and Bucher, 1998). COP9 signalosome subunit 5 (CSN5) is the catalytically competent component and contains a Jab1/MPN (**M**pr1/**P**ad1 **N**-terminal) metalloprotease domain, which is responsible for the complex's deneddylating activity (Zhang et al., 2012; Echalier et al., 2013). The signalosome is inactive without the incorporation of CSN5, and likewise, the current literature suggests CSN5 is inactive on its own and unable to deneddylate cullins in isolation (Cope et al., 2002; Sharon et al., 2009; Echalier et al., 2013; Lingaraju et al., 2014). Furthermore, CSN5 must dimerize with COP9 subunit CSN6, before the CSN5/CSN6 dimer can be incorporated into the complex and become activated (Birol et al., 2014; Lingaraju et al., 2014). Apart from COP9 subunits, CSN5 has been reported to interact with other cellular proteins (Tomoda et al., 1999; Smith et al., 2002; Yoshida et al., 2013; Shackleford and Claret, 2010) and to promote accumulation of several of its partners (Bae et al., 2002; Bemis et al., 2004; Orsborn et al., 2007; Liu et al., 2009; Lim et al., 2016). However, many of these interactions have not been extensively studied and it remains controversial whether these interactions happen within the context of the COP9 holoenzyme.

In a yeast-two hybrid screen for FBF binding partners, our lab identified *C. elegans* CSN-5 as a prominent interactor of FBF-2. The primary focus of this work is to investigate CSN-5's contribution to FBF function in the germline. We find that CSN-5 stabilizes both FBF-1 and FBF-2 in germline SPCs to promote stem cell maintenance and oogenesis, likely independent of COP9 signalosome. This finding implicates CSN-5 in supporting accumulation of stem cell regulatory proteins that we speculate is relevant to a wide range of organisms.

Results:

CSN-5 is a new interacting partner of FBFs

To identify proteins that associate with FBF-2, we performed a yeast two-hybrid screen of a *C. elegans* cDNA library with FBF-2 as bait. The screen of estimated $2x10^8$ yeast diploids identified several potential FBF-2 interactors, with one of the most abundant partners being a fragment of COP9 signalosome subunit CSN-5. To validate this potential interaction and to test whether CSN-5 might interact with FBF-1 as well as with FBF-2, we performed a directed yeast two-hybrid interaction assay, which confirmed FBF/CSN-5 association (Fig. 1B). Yeast expression of c-myc-tagged FBFs and HA-tagged CSN-5 was detected by western blot using anti-Myc and anti-HA, respectively (Fig. 1C). Additionally, we performed a GST pulldown assay with bacterially-expressed GST-tagged CSN-5 and His_6-tagged FBFs, which detected direct interaction between these proteins (Fig. 1D).

The interaction between the RNA-binding domain of FBFs and the MPN domain of CSN-5 is conserved in evolution

To elucidate the location of the interacting domains within FBFs and CSN-5, we generated several truncation constructs of FBF-1, FBF-2, and CSN-5 (Fig. 2B,D), and tested their association via GST pulldown assay. We observed that the conserved RNA-binding domains of both FBFs and the MPN domain of CSN-5 were sufficient for their interaction and binding was lost when these conserved domains were not present (Fig.

2A,C). We then tested whether FBF-2 could interact with the MPN domain of another COP9 subunit, CSN-6. GST pulldown assay suggested that the interaction of His_6::FBF-2 with GST::CSN-6^{MPN} is much weaker than that with CSN-5^{MPN} (Fig. S1A). We concluded that the FBF/CSN-5 interaction is mediated by the conserved, structured domains, with selectivity towards specific members of the domain families. We further tested whether FBF-2 interaction with MPN domains of CSN-5 and CSN-6 was RNA-dependent, and found that the binding was not disrupted by the RNase A treatment (Fig. S1B).

CSN-5 is incorporated into the COP9 signalosome protein complex as a dimer with CSN-6 (Sharon et al., 2009; Enchev et al., 2012; Birol et al., 2014). Therefore, we tested whether CSN-5 could bridge the interaction between CSN-6 and FBF-2. The ability of CSN-5 to interact with FBF-2 while bound to CSN-6 would suggest that FBF-2 might form a complex with CSN-5 in the context of COP9 signalosome. GST pulldown assays of His_6::FBF-2 with a range of GST::CSN-6^{MPN} concentrations, with or without the addition of $FLAG_3$::CSN-5^{MPN}, revealed no change in the ability of CSN-6^{MPN} to bind FBF-2 in the presence of CSN-5^{MPN} (Fig. 2E). We concluded that the interaction between FBFs and CSN-5 might take place outside of the COP9 signalosome complex.

Both FBFs and CSN-5 have homologous human proteins, PUM1/PUM2 and CSN5, respectively. We tested whether the RNA-binding domains and MPN domain of the respective human homologs (Fig. 2B,D) were able to interact. A GST pulldown assay of GST::hCSN5^{MPN} with His_6::hPUM1^{RBD} and His_6::hPUM2^{RBD} revealed that the interaction we observed for the nematode proteins is conserved for human homologs CSN5 and PUM1, but not PUM2, suggesting an evolutionarily conserved protein complex (Fig. 2F).

COP9 subunit mutants have reduced number of stem cells and the loss of *csn-5* leads to masculinization of germline

If CSN-5 facilitates FBF function in the germline, we expect *csn-5(loss-of-function, lf)* mutation to cause developmental defects similar to those caused by *fbf-1/2(lf)*. In addition to its function as a subunit of COP9 signalosome, CSN-5 interacts with other

cellular proteins and may have functions independent of the COP9 complex (Tomoda et al., 1999; Wei et al., 2008; Yoshida et al., 2013). To distinguish COP9-dependent and independent roles of CSN-5, we documented the phenotypes caused by mutations in two COP9 subunits, *csn-2* and *csn-6* in addition to *csn-5*. If the whole complex were required for specific functions, we would expect to see the same, or very similar, phenotypes across all *csn(lf)* mutants, as all mutations used in this study are expected to be null alleles (Brockway et al., 2014; Materials and Methods). Because FBF-1/2 regulate the switch from mitosis to meiosis in the *C. elegans* germline (Crittenden et al., 2002; Wickens et al., 2002) and therefore affect the size of its stem and progenitor cell (SPC) population, we quantified the number of SPCs in *csn-2(lf)*, *csn-6(lf)*, and *csn-5(lf)*. We dissected and stained adult germlines with the antibodies to a stem cell marker, REC-8, to visualize the SPC zone (Fig. 3Ai-iv; Hansen et al., 2004). We observed that all *csn(lf)* mutants had reduced numbers of SPCs compared to the wild type ($p<0.0001$, Fig. 3B) which is in general agreement with a previous report (Brockway et al., 2014). The *csn-6(lf)* and *csn-5(lf)* mutants had the most drastic reduction in SPCs, whereas the *csn-2(lf)* SPCs were less affected ($p<0.01$, Fig. 3B). This decrease in SPCs is consistent with a decrease in FBF function.

Additionally, FBFs play a role in germline sex determination by regulating the spermatogenesis to oogenesis switch (Zhang et al., 1997; Crittenden et al., 2002), so we assessed if sex determination was affected in the *csn(lf)* mutants. The majority of *csn-6(lf)* and *csn-5(lf)* mutants exhibited a masculinization of germline (Mog) phenotype, where sterile hermaphrodites produce only sperm and no oocytes (Fig. 3Ciii-iv,D). This Mog phenotype is also seen in *fbf-1/-2(lf)* mutant germlines (Crittenden et al., 2002), supporting the hypothesis that *csn-5* may be contributing to FBF function. Curiously, the *csn-2(lf)* mutant had a clearly distinct phenotype where most germlines could still form oocytes (Fig. 3Cii,D). We conclude that CSN-5 facilitates stem cell maintenance and sex determination. This new role for CSN-5 appears to be mediated by CSN-5 alone, rather than the complete COP9 signalosome complex. The distinct phenotypes of the *csn-2(lf)* mutant indicate that *csn-5(lf)* might be affecting *fbf* function independently of the signalosome.

We further hypothesized that the similar phenotypes observed in *csn-5(lf)* and *csn-6(lf)* mutants were caused by a decrease in the levels of CSN-5 protein in *csn-6(lf)*. Indeed, we observed that the levels of 3xFLAG::CSN-5 transgene in a *csn-6(lf)* background decrease by approximately 60% compared to the control (Fig. S2), similar to a previous observation of a decrease in CSN-5 levels after a knockdown of *csn-6* (Miller et al., 2009). We then tested whether increasing *csn-5* copy number in the *csn-6(lf)* mutant background through introduction of the *3xflag::csn-5* transgene would alleviate CSN-5-dependent, COP9-independent phenotypes. We find that an extra copy of *csn-5* was able to partially rescue germline masculinization of *csn-6(lf)*, resulting in phenotypes similar to those of *csn-2(lf)* (Fig. 3E). However, it was unable to rescue the low numbers of stem cells in *csn-6(lf)* (data not shown). We conclude that the role of CSN-5 in sex determination is independent of COP9 signalosome.

***csn(lf)* cause a decrease of FBF-1/2 protein levels**

We next tested whether CSN-5 function in stem cell maintenance and germline sex determination was associated with an effect on FBF proteins. In *C. elegans*, CSN-5 was previously identified as an interacting partner of germline proteins, GLH-1 and GLH-3 (Smith et al., 2002), and found to promote accumulation of GLH-1 (Orsborn et al., 2007). Therefore, we hypothesized that CSN-5 may promote FBF accumulation. We tested this hypothesis by quantifying the total FBF protein levels in the *csn(lf)* mutant worms by western blotting with the antibodies to the endogenous FBF-1 or CRISPR-tagged 3xV5::FBF-2, and using tubulin as a loading control. We found the most drastic reduction of FBF-1 protein level in *csn-5(lf)* ($p<0.005$; Fig. 4A,B) compared to the wild type, whereas *csn-6(lf)* and *csn-2(lf)* were affected weaker ($p<0.01$; $p<0.05$, respectively; Fig. 4A,B). Furthermore, FBF-1 protein levels in the *csn-5(lf)* mutant were significantly lower than those in the *csn-2(lf)* mutant ($p<0.05$; Fig. 4B). Immunostaining of the *csn-5(lf) and csn-6(lf)* mutants confirmed the loss of signal in the distal SPCs (Fig. 4C), where FBFs are normally expressed, and suggested that the reduction of FBF-1 protein does not simply result from a decrease in stem cell numbers. The stronger FBF-1 protein reduction in *csn-5(lf)* implies that CSN-5 might be promoting the accumulation

of FBF-1 independently of the COP9 complex, since the relative amounts of FBF-1 would be similar across all mutants otherwise. Additionally, we observed a significant reduction of 3xV5::FBF-2 in all *csn(lf)* mutants by western blot ($p<0.0001$; Fig. 4D,E) and confirmed this observation by immunostaining (Fig. 4F). We conclude that the steady-state levels of both FBF proteins are reduced in the *csn(lf)* mutant backgrounds.

The reduction in FBF-1/2 protein levels may be caused by a decrease in *fbf* transcripts or by an effect on FBF proteins. To start distinguishing these possibilities, we tested if *csn(lf)* affects the steady-state levels of *fbf-1/-2* mRNAs using quantitative PCR. Using *unc-54* (myosin heavy chain) as a control and normalizing mRNA abundance to a reference gene, *act-1* (actin), we observed a reduction in *fbf-1* mRNA abundance in each of the mutants but due to high variability the difference was not statistically significant. However, we observed a statistically significant reduction of *fbf-2* mRNA abundance in each *csn(lf)* mutant compared to wild type ($p<0.0001$; Fig. S3). By contrast, we did not observe a decrease in *unc-54* mRNA in any *csn(lf)* mutant (Fig. S3). As the effects of all *csn(lf)* mutants on the levels of *fbf* transcripts were similar, we conclude that COP9 signalosome is required for normal steady state levels of *fbf* mRNAs. However, distinct levels of FBF-1 protein in *csn-2(lf)* vs. *csn-5(lf)* mutant backgrounds suggest that CSN-5 might additionally promote FBF-1 protein accumulation.

***csn-5(lf)* destabilizes FBF proteins**

We then tested whether CSN-5 stabilizes FBF proteins by interfering with their proteasome-mediated degradation. If true, we expect that disruption of the proteasome function in *csn-5(lf)* mutants would restore FBF protein levels. To test this hypothesis, we knocked down *pbs-6*, a catalytic subunit of the 20S proteasome, in the *rrf-1(lf)* genetic background to preferentially direct the RNAi knockdown to the germline (Sijen et al., 2001; Kumsta and Hansen, 2012). We observed a complete rescue ($p<0.05$) of both steady-state FBF-1 and 3xV5::FBF-2 protein levels in *rrf-1(lf); csn-5(lf)* following *pbs-6(RNAi)* (Fig. 5A-D). Since we previously observed a decrease in *fbf-1/2* transcript levels in *csn-5(lf)* background (Fig. S3), we next determined whether the rescue of FBF

protein accumulation upon proteasome disruption was mediated by an increase in *fbf* mRNA abundance. Quantification of steady-state *fbf* mRNA levels by qRT-PCR revealed that *pbs-6(RNAi)* did not increase *fbf* transcript levels (Fig. 5E). We conclude that CSN-5 promotes the stability of FBF proteins.

Discussion:

In this study, we have identified the COP9 signalosome component CSN-5 as a new interacting partner of PUF-family RNA-binding proteins FBF-1 and -2, and documented COP9-independent CSN-5 function in promoting stem and progenitor cell (SPC) proliferation as well as oogenesis in *C. elegans* germline. Analysis of *csn-5(lf)* mutant background uncovered instability of FBF-1 and -2 proteins that is counteracted by CSN-5. We propose that CSN-5 exerts a COP9-independent function by maintaining steady-state levels of FBF-1 and -2 in the *C. elegans* germline (Fig. 6).

We found that the direct interaction between PUF-family proteins (FBF-1, -2, and hPUM1) and CSN5 homologs is mediated by conserved structured domains, the RNA-binding domain and the MPN domain respectively (Fig. 2A,C,F). However, not all PUF RNA-binding domains bind CSN5 and not every type of MPN domain binds PUF proteins. The RNA-binding domain of hPUM2 did not interact with the MPN domain of hCSN5 (Fig. 2F). Similar to CSN-5, CSN-6 contains an MPN domain (Birol et al., 2014). However, CSN-6's MPN domain could only bind FBF-2's RNA-binding domain at much higher concentrations than CSN-5 (Fig. S1A). Taken together, this suggests a selective association between a subset of PUF RNA-binding proteins and their specific MPN domain-containing partners. In the future, these selective interactions can help elucidate the sites mediating binding between these proteins. Intriguingly, CSN-5 appeared unable to associate with FBF-2 when in complex with CSN-6 (Fig. 2E), suggesting that this interaction takes place outside of the COP9 signalosome complex.

In line with this interpretation, we uncovered COP9-independent function of CSN-5 in *C. elegans* germline consistent with its cooperation with FBF proteins. This conclusion is supported by three lines of evidence. First, we find that *csn-5(lf*) leads to a more severe

reduction in SPC numbers than inactivation of other COP9 subunits like *csn-2* (Fig. 3A,B). Although genetic requirement for COP9 in germline mitotic cell maintenance was previously recognized (Brockway et al., 2014; Pan et al., 2014) the molecular mechanism was not identified. We now report that *csn-5* provides an additional, COP9-independent contribution to SPC maintenance through stabilizing FBFs, which are essential regulatory proteins. Second, we find that a loss of COP9-independent CSN-5 function results in germline masculinization, or failure to produce oocytes (Fig. 3C,D). By contrast, mutations of other COP9 subunits such as *csn-2(lf)* do not affect germline sex determination (Fig. 3C,D). We further uncovered that *csn-6(lf)* destabilized CSN-5 protein (Fig. S2) and thus affected both COP9-dependent and CSN-5-dependent processes in the germline. We were able to rescue CSN-5-dependent oogenesis by increasing *csn-5* copy number in *csn-6(lf)* background, providing further evidence that this process is COP9-independent (Fig. 3E). Our inability to rescue SPC numbers in *3xflag::csn-5; csn-6(lf)* background might be due to the insufficient levels of the transgenic protein as its levels are also reduced in *csn-6(lf)* compared to the wild type (Fig. S2). Third, we find that total FBF-1 protein levels are significantly depleted in *csn-5(lf)*, but are only moderately affected by *csn-2(lf)* (Fig. 4A-C). This suggests that COP9-independent CSN-5 function promotes steady state accumulation of FBF-1 protein. Our assessment of COP9-dependent effects on FBF protein levels and function is based on the phenotype of *csn-2(lf)* mutant as *csn(lf)* mutants used in this study are null-allele mutants (see Brockway et al., 2014 for *csn-5(lf)* and *csn-6(lf)*, and Fig. S4 for *csn-2(lf)* characterization). However, we have not established whether *csn-2(lf)* might affect CSN-5 protein levels and cannot exclude the possibility that some FBF-related phenotypes of *csn-2(lf)* mutant germlines result indirectly from partially compromised function of CSN-5.

Finally, we uncovered intrinsic instability of FBF proteins in *csn-5(lf)* mutant background suggesting that *csn-5* promotes FBF accumulation through protecting them from degradation. FBF protein levels in the *csn-5(lf)* genetic background were rescued by disrupting proteasome-mediated degradation without affecting *fbf* transcript levels (Fig. 5). CSN-5/hCSN5 is reported to interact with a number of proteins beyond components of the signalosome (for examples see Tomoda et al., 1999; Bae et al., 2002; Smith et

al., 2002; Yoshida et al., 2013) and to promote accumulation of some of its interacting partners (Bemis et al., 2004; Orsborn et al., 2007). Our work defines a novel class of CSN-5 interactors, the PUF-family FBF proteins that are stabilized by CSN-5 and reveals a new mechanism of CSN-5 contribution to stem cell maintenance. Based on our detection of binding between the human homologs, we speculate that hCSN5 might similarly stabilize hPUM1. The mechanism of CSN-5-dependent stabilization of its partner proteins remains unclear. One possibility suggested by previous reports in both fission yeast and mammalian cells is COP9-dependent recruitment of a **de**ub**ub**iquitinating enzyme (DUB) Ubp12p/USP15 to the complex's substrates (Zhou et al., 2003; Hetfeld et al., 2005). Importantly, in several cases DUB recruitment was shown to depend on CSN5 (Groisman et al., 2003; Wee et al., 2005; Liu et al., 2009). Alternatively, hCSN5 was reported to directly interact with HIF1α and to stabilize HIF1α in a COP9-independent manner (Bemis et al., 2004). Stabilization of HIF1α was mediated by preventing proline hydroxylation of HIF1α and by interfering with the association of hydroxylated HIF1α with pVHL ubiquitin ligase (Bemis et al., 2004). As a third option, hCSN5 metalloprotease was proposed to directly deubiquitinate its binding partner (Lim et al., 2016; Liu et al., 2020). An intriguing possibility then is that CSN5 might be able to protect FBFs from ubiquitination and thus promote their stabilization in *C. elegans* germline stem cells.

CSN-5 contribution to the regulation of germline stem cell proliferation through stabilization of FBF proteins has major implications for understanding regulatory mechanisms relevant for stem cell maintenance. Intrinsic instability of PUF-family proteins counteracted by CSN-5 might reflect a general mechanism regulating the abundance of essential stem cell factors and their effects on stem cell population dynamics. Additionally, the function of CSN-5 in FBF stabilization may be relevant for understanding cancer as hCSN5 is upregulated in many human cancers (Lee et al., 2011; Liu et al., 2020). Similarly, a number of cancers overexpress PUM1 and/or PUM2 (Guan et al., 2018; Gor et al., 2021; Shi et al., 2021; Smialek et al., 2021). This PUM protein overexpression in cancer might be borne out through its stabilization via hCSN5 and therefore reflect an unappreciated mechanism promoting cancer cell proliferation.

Materials and Methods

Nematode strains and culture

All *C. elegans* strains (Table S1) used in this study were cultured on NNGM plates seeded with OP50 as per standard protocols (Brenner, 1974).

csn-2(ok1288) allele

In order to determine the molecular nature of *csn-2(ok1288)* allele, we conducted PCR analysis of genomic DNA as well as cDNA. Total RNA isolated from *csn-2(ok1288)* hermaphrodites was reverse-transcribed using SuperScript IV reverse transcriptase (Invitrogen) and amplified with the primers AGACCCAGGAAAAGTTCGGT and GAGACCATCATCCAAAATTGCGT. Our analysis revealed that the 1680-nt genomic deletion removes most of intron 3, exon 4, and most of intron 4. The *csn-2(ok1288)* transcript is spliced from the end of exon 3 to the start of exon 5 resulting in a frameshift at amino acid 238 and a premature stop codon (removing 50% of ORF; Fig. S4). The full-length CSN-2 contains a PCI domain consisting of helical repeats 1-8 and a winged-helix (WH) subdomain, which is followed by a C-terminal alpha helix. CSN-2 is incorporated into the COP9 signalosome through association of the WH subdomain with the WH subdomains of other PCI proteins and through integration of the C-terminal helix into a bundle containing helices of all COP9 subunits (Lingaraju et al., 2014). *ok2188* deletion removes three C-terminal PCI repeats, the WH domain, and the C-terminal helix suggesting that the remaining fragment would not incorporate into COP9 signalosome.

Transgenic animals

The *3xflag::csn-5* transgene construct was generated by Gateway cloning (Thermo Fisher Scientific). The construct contains the *csn-5* promoter and genomic coding and 3'UTR sequences in pCFJ150 (Frokjaer-Jensen et al., 2008). A single-copy insertion of the transgene was generated by homologous recombination into the universal *Mos1*

insertion site on LG II after Cas9-induced double-stranded break (Dickinson et al., 2013; Wang et al., 2016). Transgene insertion was confirmed by PCR.

Yeast Two-Hybrid library screening and directed assays

For the yeast two-hybrid screen, *fbf-2* cDNA was cloned into the pGBTK vector (Clontech) and transformed into PJ68-4a yeast strain (*MAT**a** trp1-901 leu2-3,112 ura3-52 his3-200 gal4Δ gal80Δ LYS2::GAL1-HIS3 GAL2-ADE2 met2::GAL7-lacZ*; James et al., 1996). The yeast two-hybrid library was generated from the poly(A)+ mRNA isolated from mixed-stage N2 nematodes using the Matchmaker kit (Clontech) as per the manufacturer's protocol and transformed into Y1HGold strain (*MAT**α**, ura3-52, his3-200, ade2-101, trp1-901, leu2-3, 112, gal4Δ, gal80Δ, met–, MEL1*). The bait and prey library strains were mated and cultured on selective plates SD/-Trp, Leu, His, Ade with 1 mM 3-AT; the total number of screened diploids was estimated at 2.32×10^8. Out of 271 positive colonies, 99 (37%) were identified as *csn-5* fragments by PCR and sequencing of prey plasmid inserts. For directed interaction assays, FBF-1 or FBF-2 in a bait vector pGBKT7 and CSN-5 in a prey vector pGADT7 were cotransformed in PJ69-4a. Empty prey vector was used as the control. Expression of c-myc tagged FBF-1 or FBF-2 and HA tagged CSN-5 proteins in yeast colonies were confirmed by western blot, see Table S2 for antibody information. Serially diluted yeast cultures (at OD600 0.2) expressing *fbf* bait and *csn-5* prey (or empty prey) were spotted on control or the interaction selection plate SD/-Trp, -Leu, -His, -Ade (with 1mM 3-AT to inhibit leaky expression of Histidine reporter) and incubated at 30°C for 4 days.

GST pulldown assay

Expression constructs containing His_6::FBF-1 and His_6::FBF-2 have been described before (Wang et al., 2016). Truncated FBF expression constructs were generated by PCR from full-length FBF-1 or FBF-2 and inserted into pETDuet-1 plasmid (EMD Millipore). Full-length *C. elegans* CSN-5 (amino acids 1-368) and CSN-6^{MPN} (amino acids 1-197) were amplified from N2 Bristol cDNA and cloned into pGEX-KG plasmid.

Truncated CSN-5 constructs were made by PCR from full-length CSN-5 and inserted into pGEX-KG or into pFLAG-DUET (modified pETDuet-1 replacing His_6 with 3xFLAG tag) plasmids. Human $hCSN5^{MPN}$ (amino acids 1-257) was amplified from HEK293 cDNA and cloned into pGEX-KG plasmid. Human $hPUM1^{RBD}$ (isoform 1, amino acids 828-1176) and $hPUM2^{RBD}$ (isoform 3, amino acids 706-1055) were amplified from HEK293 cDNA and cloned into pETDuet-1 plasmid. All constructs were sequenced and transformed into *Escherichia coli* strain BL21(DE3) for expression. Expression of His-tagged FBF protein constructs was induced with 0.1 mM IPTG at 15°C for 20-24 hours. Expression of GST alone or GST-tagged CSN protein constructs was induced with 0.1 mM IPTG at 37°C for 4.5 hours. Pellets of induced bacteria were collected and resuspended in lysis buffer (20 mM Tris pH 7.5, 250 mM NaCl, 10% glycerol, 1 mM $MgCl_2$, 0.1% Triton X-100) containing 10 mM beta-mercaptoethanol (BME), 1 mM PMSF, 1x Roche protease inhibitor cocktail, 0.5 mg/ml lysozyme, and 6 µg/ml DNase I, rotated at 4°C for 1 hour to lyse, and cleared by centrifugation at 1110 *g* for 20 min. Cell lysate of GST alone or GST-tagged CSN constructs were bound to glutathione beads in 20 mM Tris pH 7.5, 250 mM NaCl, 10% glycerol, 0.1% Triton X-100, 10 mM BME, 1 mM PMSF, and 1x Roche protease inhibitor cocktail for 1 hour at 15°C. Binding reactions with His_6-tagged preys were incubated at 15°C for 3 hours and washed four times with 10 mM Tris pH 7.5, 150 mM NaCl, 0.1% NP-40, and 0.5 mg/ml BSA. For elution, beads were heated to 95°C for 5 minutes in sodium dodecyl sulfate (SDS) sample buffer and 10 mM dithiothreitol (DTT). To test if the FBF-2/CSN-5/-6 binding interaction is RNA-dependent, 50 µg/ml RNase A was added to His_6::FBF-2 lysate before incubation with GST alone or GST::CSN-5/-6.

Western blot analysis

Protein samples from pulldown assays were separated using Mini-PROTEAN TGX 4-20% precast gels (Bio-Rad,) and visualized using either Coomassie, stain-free chemistry, or by Western blotting. For anti-His probing, all eluates were treated the same. For anti-GST probing, GST negative control eluate was diluted 8-fold further than GST::CSN constructs to avoid overexposure. See Table S2 for antibody information.

To analyze FBF protein levels in *csn(lf)* mutants, 50 young adult worms of each genotype were picked from synchronous cultures, and lysed in SDS-PAGE sample buffer containing 2.8% SDS and 75mM DTT by boiling for 15 minutes prior to SDS-PAGE gel electrophoresis. Protein samples were separated on a 7.5% or 4-20% gel (Bio-Rad) and transferred to a 0.2 µm PVDF membrane (EMD Millipore). After transfer, membranes were blocked in 50 mM Tris pH 7.5, 180 mM NaCl, 0.05% Tween 20, and 5% non-fat dry milk powder and probed with primary antibodies (see Table S2) diluted in blocking solution. Membranes were developed using Luminata Crescendo Western HRP substrate (EMD Millipore) and visualized using Bio-Rad ChemiDoc™ MP Imaging System. Band intensities were quantified using Image Lab software version 5.1.

Immunofluorescence

Adult *C. elegans* hermaphrodites were washed in M9 and germlines were dissected on poly-L-lysine treated slides, flash frozen, and fixed for 1 minute in 100% methanol (-20°C) followed by 5 minutes in 2% paraformaldehyde/100 mM K_2HPO_4 (pH 6) at room temperature. The samples were then blocked in PBS/0.1% BSA/0.1% Tween-20 (PBS-T/BSA) for 30 minutes at room temperature. Next, samples were incubated with primary antibody diluted in PBS-T/BSA overnight at 4°C. Samples were then washed with PBS-T/BSA three times for 10 minutes each wash, before incubating with secondary antibody diluted in PBS-T/BSA for 2 hours at room temperature in a dark humid chamber. Samples were washed again three times for 10 minutes each wash before adding 10 µL Vectashield® with DAPI (Vector Laboratories) and cover-slipping. See Table S2 for antibody information. Images were acquired with a Leica DFC300G camera attached to a Leica DM5500B microscope with a 40x LP FLUOTAR NA1.3 objective using LAS X software (Leica) and stitched together using Adobe Photoshop CS3.

Phenotypic analysis

C. elegans were synchronized by bleaching and hatched L1 larvae were plated on NNGM plates with OP50 bacteria, grown at 20°C, and harvested after 96 hours. Gonads were dissected, stained for DNA with DAPI, and scored for abnormal oocytes (defined as <3 oocytes per germline, uncondensed chromosomes, endomitotic oocytes, or increased number of DAPI spots indicating achiasmatic chromosomes), masculinization of germline (Mog), and failure of gamete formation.

Germline SPC counts

C. elegans were synchronized by bleaching and hatched L1 larvae were plated on NNGM plates with OP50 bacteria, grown at 20°C, and harvested after 72 hours. Gonads were dissected and stained for mitotic marker REC-8 (Hansen et al., 2004), and the number of stem and progenitor cells was measured by counting the total number of cells positive for REC-8 staining using Cell Counter plug-in in Fiji (Schindelin et al., 2012).

RNAi treatment

The following RNAi constructs were used: *pbs-6* in pL4440 (Kamath and Ahringer, 2003). Empty vector pL4440 was used as a control in all RNAi experiments. All RNAi constructs were verified by sequencing and transformed into HT115 (DE3) *Escherichia coli*. Three colonies of freshly transformed RNAi plasmids were combined for growth in LB/75 µg/mL carbenicillin media for 4 hours, and induced with 5 mM isopropyl β-D-1-thiogalactopyranoside (IPTG) for 1 hour at 37°C. RNAi plates (NNGM containing 100 µg/mL carbenicillin and 0.4 mM IPTG) were seeded with the pelleted cells. Synchronously hatched L1 larvae were plated directly on RNAi plates, grown at 24°C, and collected for analysis after reaching adulthood.

RNA extraction and RT-qPCR

C. elegans were synchronized by bleaching and hatched L1 larvae were plated on NNGM plates with OP50 bacteria, grown at 20°C, and collected after 72 hours. 200 worms were collected per biological replicate and stored in Trizol (Invitrogen) at -80˚C. Total RNA was extracted using either Monarch Total RNA Miniprep Kit (New England Biolabs) or Direct-zol™ RNA MiniPrep kit (Zymo Research) as per manufacturers' protocols. RNA concentration was measured using Qubit (Thermo Fisher). cDNA was synthesized using the SuperScript™ IV reverse transcriptase (Invitrogen) using 300 ng RNA template per each 20 µL cDNA synthesis reaction. Quantitative PCR reactions were performed in technical triplicates per each input cDNA using iQ SYBR® Green Supermix (Bio-Rad). Primers for all targets were as previously described: *act-1* and *fbf-2* (Chauve et al., 2020), *unc-54* (Wang et al., 2020), and *fbf-1* (Voronina and Seydoux, 2010), see also Table S2. Abundance of each mRNA in *csn(lf)* mutant relative to the wild type was calculated using comparative ΔΔCt method (Plaffl, 2001) with actin *act-1* as a reference gene. After mRNA abundance of each tested gene was normalized to *act-1*, the fold change values from replicates were averaged.

Acknowledgements:

We thank members of the Voronina laboratory for helpful discussions. All research was performed at the University of Montana. Several nematode strains were provided by the *Caenorhabditis* Genetics Center, funded by the National Institutes of Health (NIH) (grant P40OD010440). *csn* knockout strains were generated by the *C. elegans* Reverse Genetics Core Facility at the University of British Columbia and Oklahoma Medical Research Foundation, both part of the international *C. elegans* Gene Knockout Consortium (Barstead et al., 2012). We are grateful to Ella Baumgarten for help with cloning. We appreciate Ariz Mohammad for sharing the modified R script (originally from the Kimble lab) and instructions on using R for cell counts.

Author Contributions:

E.O. contributed to all Figures, participated in study design, manuscript drafting and editing. M.E. provided strains, constructs, and experimental data related to Fig. 2-4, S1, and S4. X.W. provided constructs and contributed to Fig. 1, 2, and 4. M.T. and K.J. contributed strains and experimental data related to Fig. 3 and S2. E.V. contributed to generation of strains and plasmids, provided general study design, coordination, manuscript drafting and editing. All authors made manuscript revisions and approved the manuscript.

Funding:

This work was supported by NIH grants R01GM109053 to E.V. and P20GM103546 (S. Sprang, PI; E.V. Pilot Project PI), and Toelle-Bekken Family Memorial Fund Award to E.O.

Competing interests:

The authors declare no competing or financial interests.

Data availability

This study did not generate large datasets or codes, but raw data/images are available upon request.

References:

1. Austin, J., and Kimble, J. (1987). *glp-1* is required in the germ line for regulation of the decision between mitosis and meiosis in *C. elegans*. Cell, *51*, 589–599.
2. Bae, M.K., Ahn, M.Y., Jeong, J.W., Bae, M.H., Lee, Y.M., Bae, S.K., Park, J.W., Kim, K.R., and Kim, K.W. (2002). Jab1 interacts directly with HIF-1alpha and regulates its stability. J Biol Chem, *277*, 9–12.
3. Barstead, R., Moulder, G., Cobb, B., Frazee, S., Henthorn, D., Holmes, J., Jerebie, D., Landsdale, M., Osborn, J., Pritchett, C. et al. (2012). large-scale screening for targeted knockouts in the *Caenorhabditis elegans* genome. G3 (Bethesda), *2*, 1415–1425.
4. Bemis, L., Chan, D.A., Finkielstein, C.V., Qi, L., Sutphin, P.D., Chen, X., Stenmark, K., Giaccia, A.J., and Zundel, W. (2004). Distinct aerobic and hypoxic mechanisms of HIF-alpha regulation by CSN5. Genes Dev, *18*, 739–744.
5. Berry, L.W., Westlund, B., and Schedl, T. (1997). Germ-line tumor formation caused by activation of *glp-1*, a *Caenorhabditis elegans* member of the *Notch* family of receptors. Development, *124*, 925–936.
6. Birol, M., Enchev, R.I., Padilla, A., Stengel, F., Aebersold, R., Betzi, S., Yang, Y., Hoh, F., Peter, M., Dumas, C. et al. (2014). Structural and biochemical characterization of the Cop9 signalosome CSN5/CSN6 heterodimer. PLoS One, *9*, e105688.
7. Brenner, S. (1974). The genetics of *Caenorhabditis elegans*. Genetics, *77*, 71–94.
8. Brockway, H., Balukoff, N., Dean, M., Alleva, B., and Smolikove, S. (2014). The CSN/COP9 signalosome regulates synaptonemal complex assembly during meiotic prophase I of *Caenorhabditis elegans*. PLoS Genet, *10*, e1004757.
9. Buck, S.H., Chiu, D., and Saito, R.M. (2009). The cyclin-dependent kinase inhibitors, *cki-1* and *cki-2*, act in overlapping but distinct pathways to control cell cycle quiescence during *C. elegans* development. Cell Cycle, *8*, 2613–2620.
10. Chamovitz, D.A. (2009). Revisiting the COP9 signalosome as a transcriptional regulator. EMBO Rep, *10*, 352–358.

11. Chamovitz, D.A., Wei, N., Osterlund, M.T., von Arnim, A.G., Staub, J.M., Matsui, M., and Deng, X.W. (1996). The COP9 complex, a novel multisubunit nuclear regulator involved in light control of a plant developmental switch. Cell, *86*, 115–121.
12. Chauve, L., Le Pen, J., Hodge, F., Todtenhaupt, P., Biggins, L., Miska, E.A., Andrews, S., and Casanueva, O. (2020). High-Throughput Quantitative RT-PCR in Single and Bulk C. elegans Samples Using Nanofluidic Technology. J Vis Exp, *159*, e61132
13. Chen, J., Mohammad, A., Pazdernik, N., Huang, H., Bowman, B., Tycksen, E., and Schedl, T. (2020). GLP-1 Notch-LAG-1 CSL control of the germline stem cell fate is mediated by transcriptional targets *lst-1* and *sygl-1*. PLoS Genet, *16*, e1008650.
14. Claret, F.X., Hibi, M., Dhut, S., Toda, T., and Karin, M. (1996). A new group of conserved coactivators that increase the specificity of AP-1 transcription factors. Nature, *383*, 453–457.
15. Cope, G.A., Suh, G.S., Aravind, L., Schwarz, S.E., Zipursky, S.L., Koonin, E.V., and Deshaies, R.J. (2002). Role of predicted metalloprotease motif of Jab1/Csn5 in cleavage of Nedd8 from Cul1. Science, *298*, 608–611.
16. Crittenden, S.L., Bernstein, D.S., Bachorik, J.L., Thompson, B.E., Gallegos, M., Petcherski, A.G., Moulder, G., Barstead, R., Wickens, M., and Kimble, J. (2002). A conserved RNA-binding protein controls germline stem cells in *Caenorhabditis elegans*. Nature, *417*, 660–663.
17. Demarco, R.S., Stack, B.J., Tang, A.M., Voog, J., Sandall, S.L., Southall, T.D., Brand, A.H., and Jones, D.L. (2022). Escargot controls somatic stem cell maintenance through the attenuation of the insulin receptor pathway in *Drosophila*. Cell Rep, *39*, 110679.
18. Dessau, M., Halimi, Y., Erez, T., Chomsky-Hecht, O., Chamovitz, D.A., and Hirsch, J.A. (2008). The *Arabidopsis* COP9 signalosome subunit 7 is a model PCI domain protein with subdomains involved in COP9 signalosome assembly. Plant Cell, *20*, 2815–2834.

19. Dickinson, D.J., Ward, J.D., Reiner, D.J., and Goldstein, B. (2013). Engineering the *Caenorhabditis elegans* genome using Cas9-triggered homologous recombination. Nat Methods, *10*, 1028–1034.
20. Doronkin, S., Djagaeva, I., and Beckendorf, S.K. (2003). The COP9 signalosome promotes degradation of Cyclin E during early *Drosophila* oogenesis. Dev Cell, *4*, 699–710.
21. Echalier, A., Pan, Y., Birol, M., Tavernier, N., Pintard, L., Hoh, F., Ebel, C., Galophe, N., Claret, F.X., and Dumas, C. (2013). Insights into the regulation of the human COP9 signalosome catalytic subunit, CSN5/Jab1. Proc Natl Acad Sci U S A, *110*, 1273–1278.
22. Enchev, R.I., Scott, D.C., da Fonseca, P.C., Schreiber, A., Monda, J.K., Schulman, B.A., Peter, M., and Morris, E.P. (2012). Structural basis for a reciprocal regulation between SCF and CSN. Cell Rep, *2*, 616–627.
23. Frøkjaer-Jensen, C., Davis, M.W., Hopkins, C.E., Newman, B.J., Thummel, J.M., Olesen, S.P., Grunnet, M., and Jorgensen, E.M. (2008). Single-copy insertion of transgenes in *Caenorhabditis elegans*. Nat Genet, *40*, 1375–1383.
24. Gor, R., Sampath, S.S., Lazer, L.M., and Ramalingam, S. (2021). RNA binding protein PUM1 promotes colon cancer cell proliferation and migration. Int J Biol Macromol, *174*, 549–561.
25. Groisman, R., Polanowska, J., Kuraoka, I., Sawada, J., Saijo, M., Drapkin, R., Kisselev, A.F., Tanaka, K., and Nakatani, Y. (2003). The ubiquitin ligase activity in the DDB2 and CSA complexes is differentially regulated by the COP9 signalosome in response to DNA damage. Cell, *113*, 357–367.
26. Guan, X., Chen, S., Liu, Y., Wang, L.L., Zhao, Y., and Zong, Z.H. (2018). PUM1 promotes ovarian cancer proliferation, migration and invasion. Biochem Biophys Res Commun, *497*, 313–318.
27. Hansen, D., Hubbard, E.J., and Schedl, T. (2004). Multi-pathway control of the proliferation versus meiotic development decision in the *Caenorhabditis elegans* germline. Dev Biol, *268*, 342–357.
28. Hetfeld, B.K., Helfrich, A., Kapelari, B., Scheel, H., Hofmann, K., Guterman, A., Glickman, M., Schade, R., Kloetzel, P.M., and Dubiel, W. (2005). The zinc finger

of the CSN-associated deubiquitinating enzyme USP15 is essential to rescue the E3 ligase Rbx1. Curr Biol, *15*, 1217–1221.

29. Hofmann, K., and Bucher, P. (1998). The PCI domain: a common theme in three multiprotein complexes. Trends Biochem Sci, *23*, 204–205.
30. Hubbard, E.J. (2007). *Caenorhabditis elegans* germ line: a model for stem cell biology. Dev Dyn, *236*, 3343–3357.
31. James, P., Halladay, J., and Craig, E.A. (1996). Genomic libraries and a host strain designed for highly efficient two-hybrid selection in yeast. Genetics, *144*, 1425–1436.
32. Kalchhauser, I., Farley, B.M., Pauli, S., Ryder, S.P., and Ciosk, R. (2011). FBF represses the Cip/Kip cell-cycle inhibitor CKI-2 to promote self-renewal of germline stem cells in *C. elegans*. EMBO J, *30*, 3823–3829.
33. Kamath, R.S., and Ahringer, J. (2003). Genome-wide RNAi screening in *Caenorhabditis elegans*. Methods, *30*, 313–321.
34. Kimble, J., and Crittenden, S.L. (2007). Controls of germline stem cells, entry into meiosis, and the sperm/oocyte decision in *Caenorhabditis elegans*. Annu Rev Cell Dev Biol, *23*, 405–433.
35. Kimble, J.E., and White, J.G. (1981). On the control of germ cell development in *Caenorhabditis elegans*. Dev Biol, *81*, 208–219.
36. Kumsta, C., and Hansen, M. (2012). *C. elegans rrf-1* mutations maintain RNAi efficiency in the soma in addition to the germline. PLoS One, *7*, e35428.
37. Lee, C., Sorensen, E.B., Lynch, T.R., and Kimble, J. (2016). *C. elegans* GLP-1/Notch activates transcription in a probability gradient across the germline stem cell pool. eLife, *5*, e18370.
38. Lee, M.H., Zhao, R., Phan, L., and Yeung, S.C. (2011). Roles of COP9 signalosome in cancer. Cell Cycle, *10*, 3057–3066.
39. Lim, S.O., Li, C.W., Xia, W., Cha, J.H., Chan, L.C., Wu, Y., Chang, S.S., Lin, W.C., Hsu, J.M., Hsu, Y.H. et al. (2016). Deubiquitination and Stabilization of PD-L1 by CSN5. Cancer Cell, *30*, 925–939.

40. Lingaraju, G.M., Bunker, R.D., Cavadini, S., Hess, D., Hassiepen, U., Renatus, M., Fischer, E.S., and Thomä, N.H. (2014). Crystal structure of the human COP9 signalosome. Nature, *512*, 161–165.
41. Liu, Y., Shah, S.V., Xiang, X., Wang, J., Deng, Z.B., Liu, C., Zhang, L., Wu, J., Edmonds, T., Jambor, C. et al. (2009). COP9-associated CSN5 regulates exosomal protein deubiquitination and sorting. Am J Pathol, *174*, 1415–1425.
42. Liu, C., Yao, Z., Wang, J., Zhang, W., Yang, Y., Zhang, Y., Qu, X., Zhu, Y., Zou, J., Peng, S. et al. (2020). Macrophage-derived CCL5 facilitates immune escape of colorectal cancer cells via the p65/STAT3-CSN5-PD-L1 pathway. Cell Death Differ, *27*, 1765–1781.
43. Lyapina, S., Cope, G., Shevchenko, A., Serino, G., Tsuge, T., Zhou, C., Wolf, D.A., Wei, N., Shevchenko, A., and Deshaies, R.J. (2001). Promotion of NEDD-CUL1 conjugate cleavage by COP9 signalosome. Science, *292*, 1382–1385.
44. Miller, R.K., Qadota, H., Stark, T.J., Mercer, K.B., Wortham, T.S., Anyanful, A., and Benian, G.M. (2009). CSN-5, a component of the COP9 signalosome complex, regulates the levels of UNC-96 and UNC-98, two components of M-lines in *Caenorhabditis elegans* muscle. Mol Biol Cell, *20*, 3608–3616.
45. Morrison, S.J., Shah, N.M., and Anderson, D.J. (1997). Regulatory mechanisms in stem cell biology. Cell, *88*, 287–298.
46. Orsborn, A.M., Li, W., McEwen, T.J., Mizuno, T., Kuzmin, E., Matsumoto, K., and Bennett, K.L. (2007). GLH-1, the *C. elegans* P granule protein, is controlled by the JNK KGB-1 and by the COP9 subunit CSN-5. Development, *134*, 3383–3392.
47. Pan, L., Wang, S., Lu, T., Weng, C., Song, X., Park, J.K., Sun, J., Yang, Z., Yu, J., Tang, H., et al. (2014). Protein competition switches the function of COP9 from self-renewal to differentiation. Nature, *514*, 233-236.
48. Pazdernik, N., and Schedl, T. (2013). Introduction to germ cell development in *Caenorhabditis elegans*. Adv Exp Med Biol, *757*, 1–16.
49. Pfaffl, M.W. (2001). A new mathematical model for relative quantification in real-time RT-PCR. Nucleic Acids Res, *29*, e45.

50. Pintard, L., Kurz, T., Glaser, S., Willis, J.H., Peter, M., and Bowerman, B. (2003). Neddylation and deneddylation of CUL-3 is required to target MEI-1/Katanin for degradation at the meiosis-to-mitosis transition in *C. elegans*. Curr Biol, *13*, 911–921.
51. Prasad, A., Porter, D.F., Kroll-Conner, P.L., Mohanty, I., Ryan, A.R., Crittenden, S.L., Wickens, M., and Kimble, J. (2016). The PUF binding landscape in metazoan germ cells. RNA, *22*, 1026–1043.
52. Qin, N., Xu, D., Li, J., and Deng, X.W. (2020). COP9 signalosome: Discovery, conservation, activity, and function. J Integr Plant Biol, *62*, 90–103.
53. Samuels, T.J., Järvelin, A.I., Ish-Horowicz, D., and Davis, I. (2020). Imp/IGF2BP levels modulate individual neural stem cell growth and division through. eLife, *9*, e51529.
54. Schindelin, J., Arganda-Carreras, I., Frise, E., Kaynig, V., Longair, M., Pietzsch, T., Preibisch, S., Rueden, C., Saalfeld, S., Schmid, B. et al. (2012). Fiji: an open-source platform for biological-image analysis. Nat Methods, *9*, 676–682.
55. Shackleford, T.J., and Claret, F.X. (2010). JAB1/CSN5: a new player in cell cycle control and cancer. Cell Div, *5*, 26.
56. Sharon, M., Mao, H., Boeri Erba, E., Stephens, E., Zheng, N., and Robinson, C.V. (2009). Symmetrical modularity of the COP9 signalosome complex suggests its multifunctionality. Structure, *17*, 31–40.
57. Shi, P., Zhang, J., Li, X., Li, W., Li, H., and Fu, P. (2021). Long non-coding RNA NORAD inhibition upregulates microRNA-323a-3p to suppress tumorigenesis and development of breast cancer through the PUM1/eIF2 axis. Cell Cycle, *20*, 1295–1307.
58. Shin, H., Haupt, K.A., Kershner, A.M., Kroll-Conner, P., Wickens, M., and Kimble, J. (2017). SYGL-1 and LST-1 link niche signaling to PUF RNA repression for stem cell maintenance in *Caenorhabditis elegans*. PLoS Genet, *13*, e1007121.
59. Sijen, T., Fleenor, J., Simmer, F., Thijssen, K.L., Parrish, S., Timmons, L., Plasterk, R.H., and Fire, A. (2001). On the role of RNA amplification in dsRNA-triggered gene silencing. Cell, *107*, 465–476.

60. Smialek, M.J., Ilaslan, E., Sajek, M.P., and Jaruzelska, J. (2021). Role of PUM RNA-binding proteins in cancer. Cancers (Basel), *13*, 129.
61. Smith, P., Leung-Chiu, W.M., Montgomery, R., Orsborn, A., Kuznicki, K., Gressman-Coberly, E., Mutapcic, L., and Bennett, K. (2002). The GLH proteins, *Caenorhabditis elegans* P granule components, associate with CSN-5 and KGB-1, proteins necessary for fertility, and with ZYX-1, a predicted cytoskeletal protein. Dev Biol, *251*, 333–347.
62. Suh, N., Crittenden, S.L., Goldstrohm, A., Hook, B., Thompson, B., Wickens, M., and Kimble, J. (2009). FBF and its dual control of *gld-1* expression in the *Caenorhabditis elegans* germline. Genetics, *181*, 1249–1260.
63. Tomoda, K., Kubota, Y., and Kato, J. (1999). Degradation of the cyclin-dependent-kinase inhibitor p27Kip1 is instigated by Jab1. Nature, *398*, 160–165.
64. Vogiatzoglou, A.P., Moretto, F., Makkou, M., Papamatheakis, J., and Kretsovali, A. (2022). Promyelocytic leukemia protein (PML) and stem cells: from cancer to pluripotency. Int J Dev Biol, *66*, 85–95.
65. Voronina, E., and Greenstein, D. (2016). Germ cell fate determination in *C. elegans*. In eLS, John Wiley & Sons, Ltd: Chichester 1-8.
66. Voronina, E., and Seydoux, G. (2010). The *C. elegans* homolog of nucleoporin Nup98 is required for the integrity and function of germline P granules. Development, *137*, 1441–1450.
67. Voronina, E., Paix, A., and Seydoux, G. (2012). The P granule component PGL-1 promotes the localization and silencing activity of the PUF protein FBF-2 in germline stem cells. Development, *139*, 3732–3740.
68. Wang, X., and Voronina, E. (2020). Diverse roles of PUF proteins in germline stem and progenitor cell development in *C. elegans*. Front Cell Dev Biol, *8*, 29.
69. Wang, X., Ellenbecker, M., Hickey, B., Day, N.J., Osterli, E., Terzo, M., and Voronina, E. (2020). Antagonistic control of *Caenorhabditis elegans* germline stem cell proliferation and differentiation by PUF proteins FBF-1and FBF-2. eLife, *9*, e52788.

70. Wang, X., Olson, J.R., Rasoloson, D., Ellenbecker, M., Bailey, J., and Voronina, E. (2016). Dynein light chain DLC-1 promotes localization and function of the PUF protein FBF-2 in germline progenitor cells. Development, *143*, 4643–4653.
71. Wee, S., Geyer, R.K., Toda, T., and Wolf, D.A. (2005). CSN facilitates Cullin-RING ubiquitin ligase function by counteracting autocatalytic adapter instability. Nat Cell Biol, *7*, 387–391.
72. Wei, N., and Deng, X.W. (1992). COP9: a new genetic locus involved in light-regulated development and gene expression in *Arabidopsis*. Plant Cell, *4*, 1507–1518.
73. Wei, N., Chamovitz, D.A., and Deng, X.W. (1994). *Arabidopsis* COP9 is a component of a novel signaling complex mediating light control of development. Cell, *78*, 117–124.
74. Wei, N., Serino, G., and Deng, X.W. (2008). The COP9 signalosome: more than a protease. Trends Biochem Sci, *33*, 592–600.
75. Wickens, M., Bernstein, D.S., Kimble, J., and Parker, R. (2002). A PUF family portrait: 3'UTR regulation as a way of life. Trends Genet, *18*, 150–157.
76. Wu, J.T., Lin, H.C., Hu, Y.C., and Chien, C.T. (2005). Neddylation and deneddylation regulate Cul1 and Cul3 protein accumulation. Nat Cell Biol, *7*, 1014–1020.
77. Yoshida, A., Yoneda-Kato, N., and Kato, J.Y. (2013). CSN5 specifically interacts with CDK2 and controls senescence in a cytoplasmic cyclin E-mediated manner. Sci Rep, *3*, 1054.
78. Zhang, B., Gallegos, M., Puoti, A., Durkin, E., Fields, S., Kimble, J., and Wickens, M.P. (1997). A conserved RNA-binding protein that regulates sexual fates in the *C. elegans* hermaphrodite germ line. Nature, *390*, 477–484.
79. Zhang, H., Gao, Z.Q., Wang, W.J., Liu, G.F., Shtykova, E.V., Xu, J.H., Li, L.F., Su, X.D., and Dong, Y.H. (2012). The crystal structure of the MPN domain from the COP9 signalosome subunit CSN6. FEBS Lett, *586*, 1147–1153.
80. Zhou, C., Wee, S., Rhee, E., Naumann, M., Dubiel, W., and Wolf, D.A. (2003). Fission yeast COP9/signalosome suppresses cullin activity through recruitment of the deubiquitylating enzyme Ubp12p. Mol Cell, *11*, 927–938.

Figure Legends:

Fig. 1. CSN-5 interacts with FBFs. (A) Schematic of adult *C. elegans* hermaphrodite (bottom) with a focus on posterior gonadal arm (bottom, boxed in red; top). Stem and progenitor cells (SPCs) expressing FBF proteins are highlighted in green. COP9 subunit CSN-5 is expressed throughout oogenic germline. (B) Interaction between CSN-5 and FBF-1/-2 is detected in a yeast two-hybrid assay (Y2H) with FBFs as baits and CSN-5 as prey. This experiment was performed in two replicates. (C) Western blot confirming expression of FBFs and CSN-5 in yeast cultures. (D) GST pulldown assay detects a direct interaction between GST::CSN-5 and both His_6::FBF-1 and His_6::FBF-2. FBFs are detected by Western blot with anti-His. Total protein seen by stain-free chemistry, the position of GST::CSN-5 is marked with a black dot.

Fig. 2. Interaction between the FBF RNA-binding domain and the MPN domain of CSN-5 is conserved in evolution. (A) GST pulldown of GST::CSN-5 with His_6::FBF-1^{RBD}, His_6::FBF-2^{RBD}, His_6::FBF-$2^{N\text{-}term}$ constructs as detected by western blot with anti-His and anti-GST, the position of GST::CSN-5 is marked with a black dot. (B) FBF-1/-2 and hPUM1/2 truncation constructs. Grey: RNA-binding domain. Amino acid positions of the truncations are indicated above each construct. (C) GST pulldown of GST::CSN-5 constructs with His_6::FBF-2 as detected by western blot with anti-His and anti-GST, the positions of GST-tagged constructs are marked with a black dot. (D) CSN-5, CSN-6, and hCSN5 truncation constructs. Brown: core MPN domain. C-terminal helices (purple ovals) that incorporate into the helical bundle of the COP9 signalosome (Lingaraju et al., 2014). Amino acid positions of the truncations are indicated above each construct. (E) GST pulldown assay of His_6::FBF-2 with increasing concentrations of GST::CSN-6^{MPN}, with or without the addition of $FLAG_3$::CSN-5^{MPN} as detected by western blot with anti-His or anti-FLAG. Total protein seen by Coomassie. See also Fig. S1. (F) GST pulldown of human homologs, GST::hCSN5^{MPN} with His_6::hPUM1^{RBD} or His_6::hPUM2^{RBD}, as detected by western blot with anti-His and anti-GST.

Fig. 3. COP9 subunit mutants have reduced number of stem cells and both mutants of *csn-5* and *csn-6* exhibit masculinization of germline. (Ai-iv) Distal germlines dissected from adult *3xv5::fbf-2(q932)*, referred to as wild type, and

respective *3xv5::fbf-2(q932); csn(lf)* mutants were stained with anti-REC-8 (green) to visualize SPC zone. Germlines are outlined with dashed lines and vertical dotted lines indicate the SPC zone boundary. Scale bars: 10 µm. (B) Quantification of SPCs in wild type and *csn(lf)* mutants. Differences in number of SPCs was evaluated by one-way ANOVA with Tukey's post-test. Grey asterisks denote statistical significance compared to wild type (****, $p<0.0001$) and blue asterisks denote statistical significance compared to *csn-2(lf)* (**, $p<0.01$). Number of germlines scored (*N*) are indicated at the bottom of the graph. Stem cell quantification reflects six biological replicates of wild type and three biological replicates for each *csn(lf)* mutant. (Ci-iv) Gonads of adult wild type and respective *csn(lf)* mutants dissected and stained for DNA with DAPI. Arrows indicate gametes. Germlines are outlined with dashed lines. Scale bars: 10 µm. (D) Gametogenesis in wild type and *csn(lf)* mutants. Number of germlines scored (*N*) are indicated at the top of each column. Data are plotted in aggregate and reflect six biological replicates of wild type, four replicates of *csn-6(lf)*, and three replicates of each *csn-2(lf)* and *csn-5(lf)*. (E) Masculinization of *csn-6(lf)* is partially rescued by an extra copy of *csn-5* gene in *3xflag::csn-5; csn-6(lf)* strain. Number of germlines scored (*N*) are indicated at the top of the graph. Data are plotted in aggregate and reflect three biological replicates. See also Fig. S2.

Fig. 4. FBF-1/-2 protein levels are reduced in *csn(lf)* mutants. (A,D) Western blot analysis of *3xv5::fbf-2(q932); csn(lf)* mutant worm lysate reveals reduced levels of (A) FBF-1 and (D) 3xV5::FBF-2. Tubulin is used as a loading control. Endogenous FBF-1 and CRISPR-tagged 3xV5::FBF-2 are detected by anti-FBF-1 and anti-V5. (B,E) Total FBF protein level of each *3xv5::fbf-2(q932); csn(lf)* mutant normalized to *3xv5::fbf-2(q932)*, referred to here as wild type. Differences in protein level were evaluated by one-way ANOVA with Tukey's post-test. Grey asterisks denote statistical significance compared to wild type and blue bracket and asterisk denote statistical significance compared to *csn-2(lf)* (*, $p<0.05$; **, $p<0.01$; ***, $p<0.005$; ****, $p<0.0001$). Number of biological replicates (*N*) is indicated at the bottom of the graphs. Mean group values are shown as lines and error bars denote standard deviation. (C,F) Gonads of *csn(lf)* mutants are dissected and stained with (C) anti-FBF-1 (green) or (F) anti-V5 (green) and DAPI (blue) to visualize protein levels of FBF-1/-2. The individual FBF (green) and

DAPI (greyscale) channels are also shown for better contrast. Germlines are outlined with dashed lines and vertical dotted lines indicate border of the SPC zone. Scale bars: 10 µm.

Fig. 5. *csn-5(lf)* destabilizes FBF proteins. (A,C) FBF protein levels after treatment with a control RNAi and *pbs-6(RNAi)* in *rrf-1(lf); 3xv5::fbf-2(q932)*, referred to as wild type here, and *rrf-1(lf); 3xv5::fbf-2(q932); csn-5(lf)*, referred to as *csn-5(ok1064)*. (A) Endogenous FBF-1 and (C) CRISPR-tagged 3xV5::FBF-2 are detected by anti-FBF-1 and anti-V5. Tubulin is used as a loading control. (B,D) Total FBF protein levels of *csn-5(lf)* normalized to wild type control RNAi. Control RNAi is shown as the leftmost darker bar for each genetic background and *pbs-6(RNAi)* is shown as the lighter corresponding shade on the right. Difference in FBF protein level was evaluated by one-way ANOVA with Sidak's post-test. Grey bracket with asterisks denotes statistical significance compared to wild type control RNAi (**, $p<0.01$) and red brackets with asterisks denote statistical significance compared to *csn-5(lf)* control RNAi (*, $p<0.05$). Number of biological replicates (*N*) is indicated below the graph, mean value is indicated as a line and error bars denote standard deviation. (E) Steady-state levels of transcripts indicated on the X-axis are quantified by RT-qPCR and normalized to reference gene *act-1*; *unc-54* is a control. Differences in relative mRNA abundance of *fbf-1/-2* was evaluated by one-way ANOVA with Dunnett's post-test. Asterisks denote statistical significance compared to wild type control RNAi (**, $p<0.01$; ***, $p<0.005$; ****, $p<0.0001$). The data reflect four biological replicates of control RNAi for wild type and *csn-5(ok1064),* three replicates of wild type; *pbs-6(RNAi)*, and two replicates of *csn-5(ok1064); pbs-6(RNAi)*. Mean values are plotted as lines with error bars representing standard deviation.

Fig. 6. A model of CSN-5 stabilizing FBFs. (A) CSN-5 promotes the stability of FBFs, thereby allowing FBFs proteins to maintain the SPC zone and enable the switch from spermatogenesis to oogenesis. (B) Intrinsically unstable FBF proteins are readily degraded by the proteasome resulting in a germline with fewer SPCs and no female gametes in the absence of CSN-5.

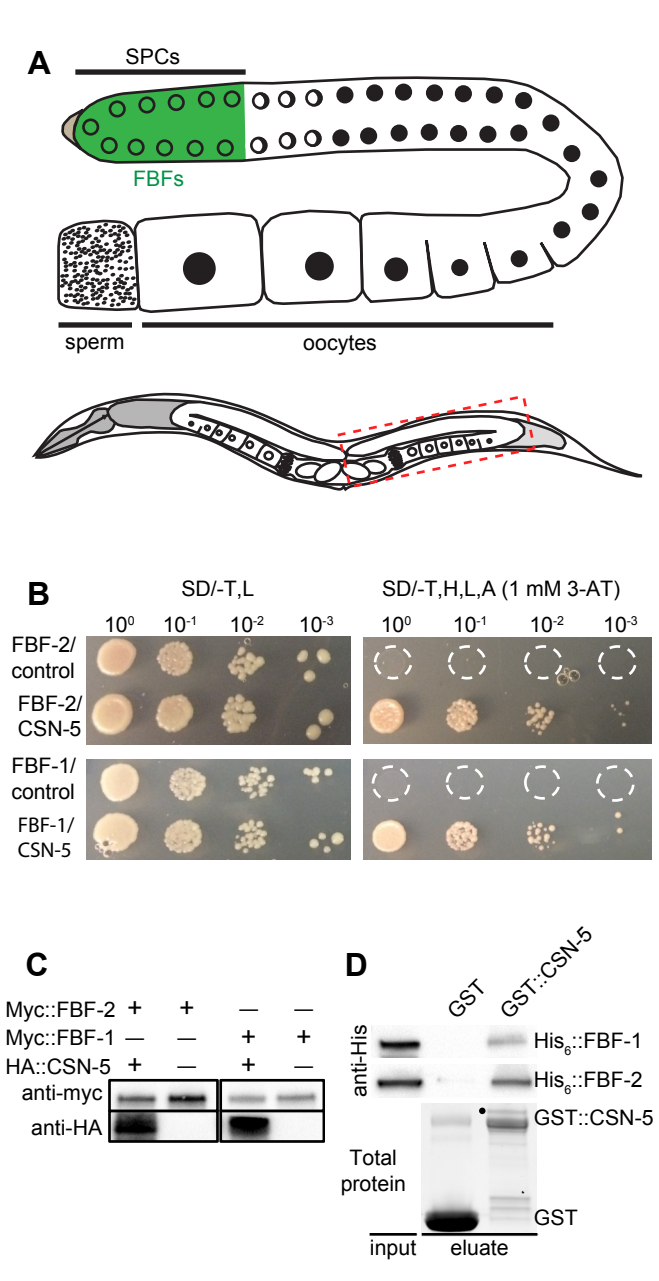
A
SPCs
FBFs
sperm
oocytes
B
SD/-T,L
SD/-T,H,L,A (1 mM 3-AT)
10^0
10^-1
10^-2
10^-3
FBF-2/ control
FBF-2/ CSN-5
FBF-1/ control
FBF-1/ CSN-5
C
Myc::FBF-2 + + — —
Myc::FBF-1 — — + +
HA::CSN-5 + — + —
anti-myc
anti-HA
D
GST
GST::CSN-5
anti-His
His6::FBF-1
His6::FBF-2
GST::CSN-5
Total protein
GST
input
eluate

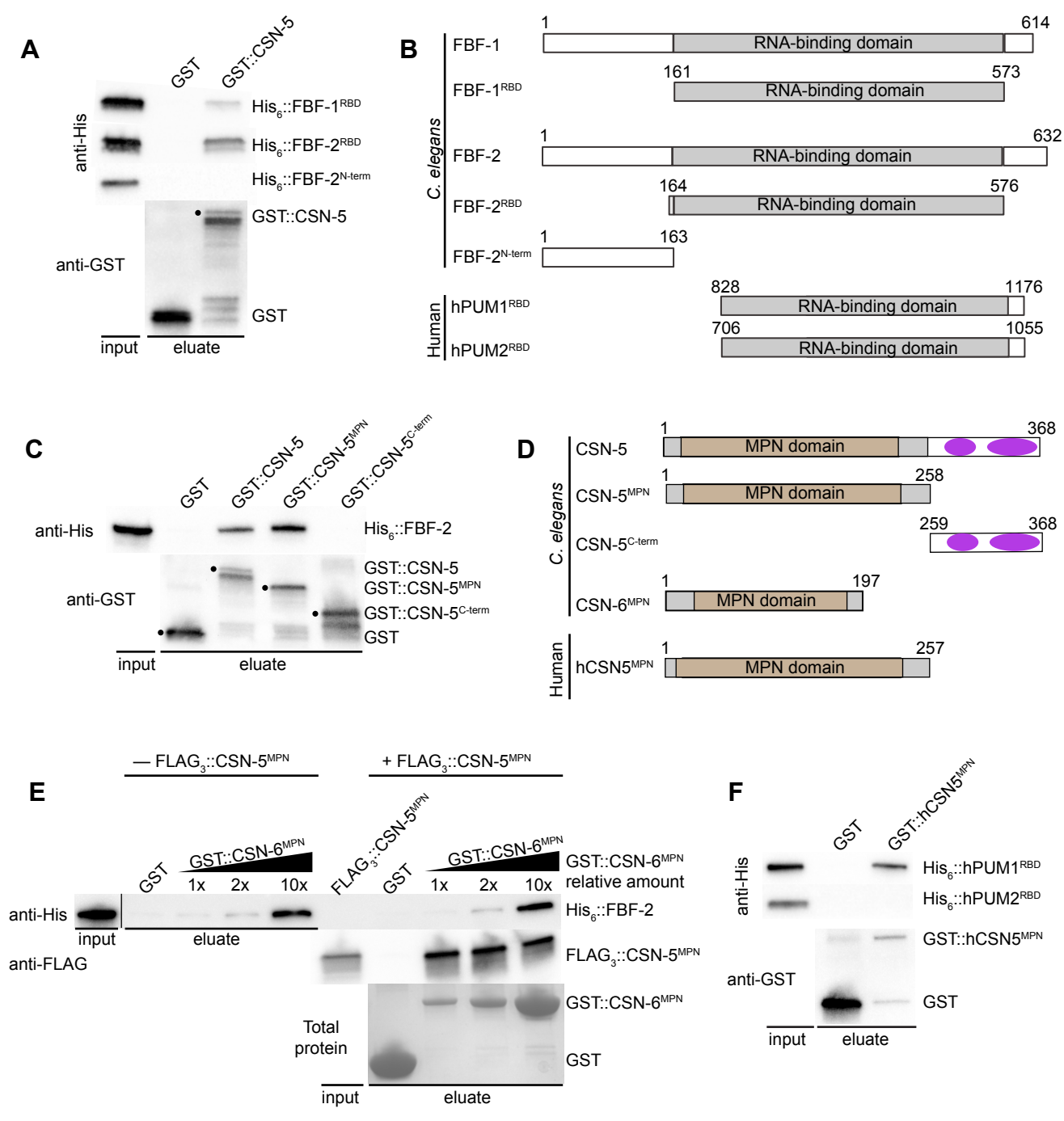
A
GST
GST::CSN-5
anti-His
His6::FBF-1RBD
His6::FBF-2RBD
His6::FBF-2N-term
GST::CSN-5
anti-GST
GST
input
eluate
B
C. elegans
FBF-1
1
614
RNA-binding domain
FBF-1RBD
161
573
RNA-binding domain
FBF-2
1
632
RNA-binding domain
FBF-2RBD
164
576
RNA-binding domain
FBF-2N-term
1
163
Human
hPUM1RBD
828
1176
RNA-binding domain
hPUM2RBD
706
1055
RNA-binding domain
C
GST
GST::CSN-5
GST::CSN-5MPN
GST::CSN-5C-term
anti-His
His6::FBF-2
anti-GST
GST::CSN-5
GST::CSN-5MPN
GST::CSN-5C-term
GST
input
eluate
D
C. elegans
CSN-5
1
368
MPN domain
CSN-5MPN
1
258
MPN domain
CSN-5C-term
259
368
CSN-6MPN
1
197
MPN domain
Human
hCSN5MPN
1
257
MPN domain
E
— FLAG3::CSN-5MPN
+ FLAG3::CSN-5MPN
GST
GST::CSN-6MPN
1x
2x
10x
FLAG3::CSN-5MPN
GST
GST::CSN-6MPN
1x
2x
10x
GST::CSN-6MPN relative amount
anti-His
His6::FBF-2
input
eluate
anti-FLAG
FLAG3::CSN-5MPN
GST::CSN-6MPN
Total protein
GST
input
eluate
F
GST
GST::hCSN5MPN
anti-His
His6::hPUM1RBD
His6::hPUM2RBD
GST::hCSN5MPN
anti-GST
GST
input
eluate

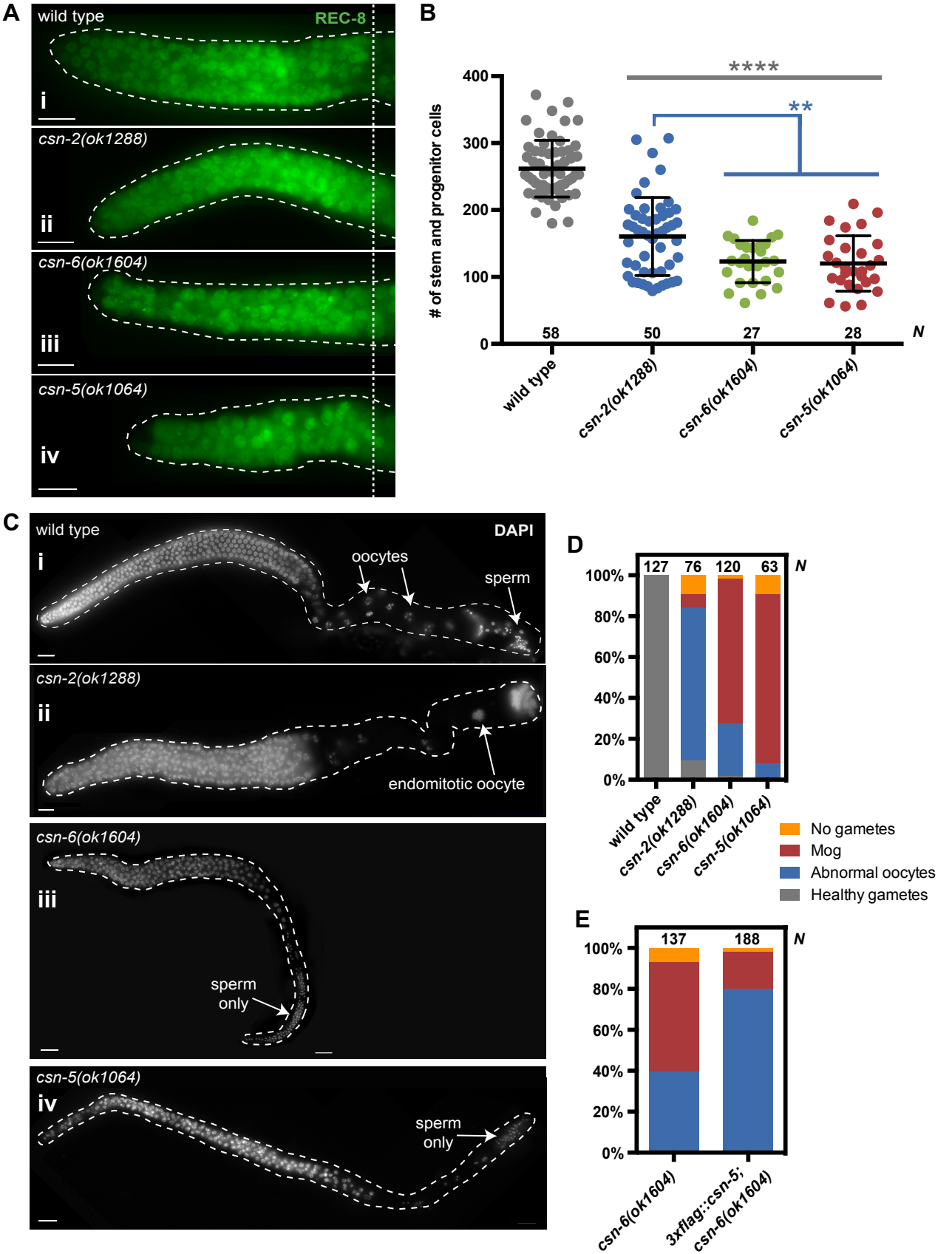
A
wild type
REC-8
i
csn-2(ok1288)
ii
csn-6(ok1604)
iii
csn-5(ok1064)
iv
B
****
**
# of stem and progenitor cells
400
300
200
100
0
58
50
27
28
N
wild type
csn-2(ok1288)
csn-6(ok1604)
csn-5(ok1064)
C
wild type
DAPI
i
oocytes
sperm
csn-2(ok1288)
ii
endomitotic oocyte
csn-6(ok1604)
iii
sperm
only
csn-5(ok1064)
iv
sperm
only
D
127
76
120
63
N
100%
80%
60%
40%
20%
0%
wild type
csn-2(ok1288)
csn-6(ok1604)
csn-5(ok1064)
No gametes
Mog
Abnormal oocytes
Healthy gametes
E
137
188
N
100%
80%
60%
40%
20%
0%
csn-6(ok1604)
3xflag::csn-5;
csn-6(ok1604)

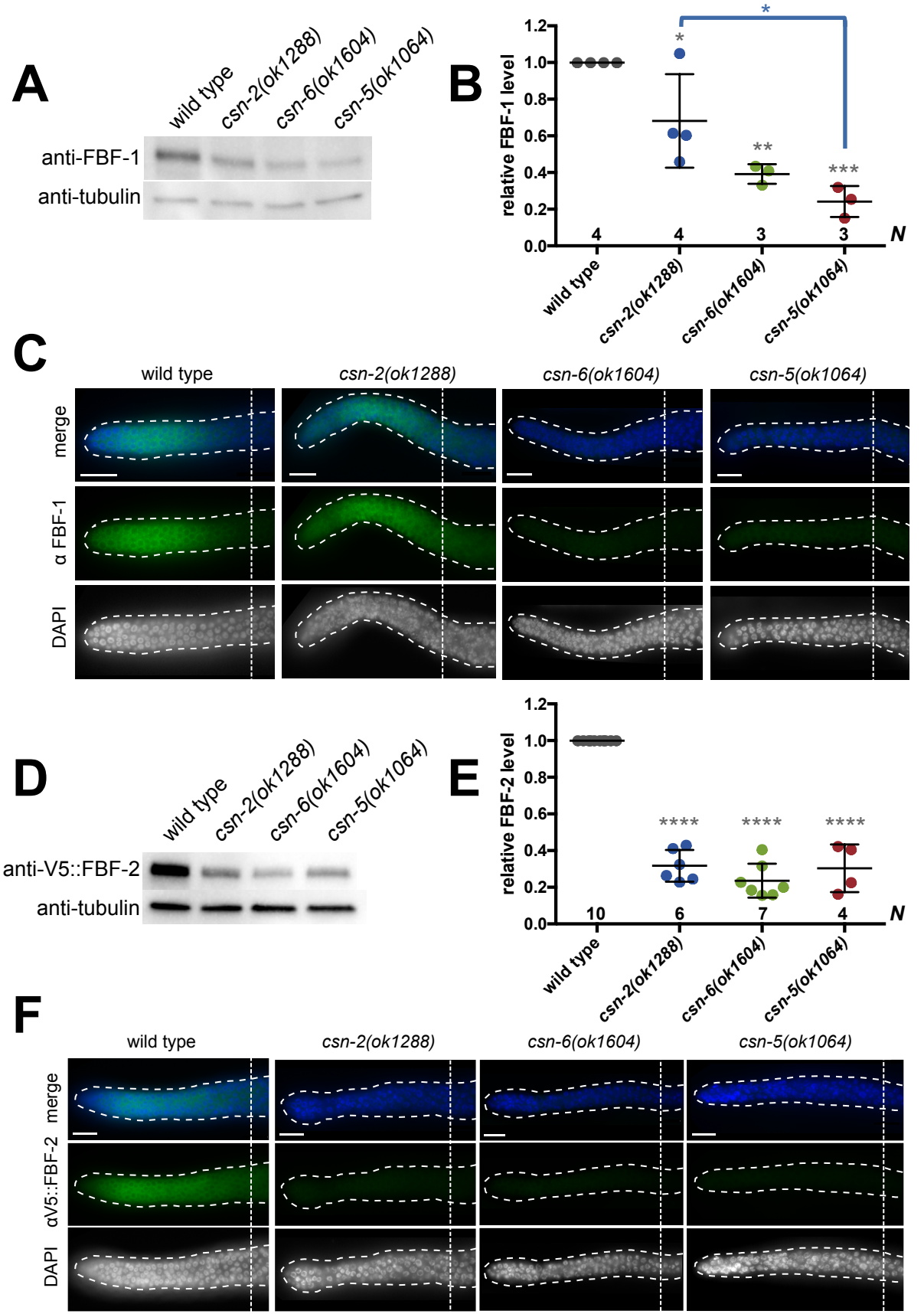
A
wild type
csn-2(ok1288)
csn-6(ok1604)
csn-5(ok1064)
anti-FBF-1
anti-tubulin
B
relative FBF-1 level
1.2
1.0
0.8
0.6
0.4
0.2
0.0
*
*
**
***
4
4
3
3
N
wild type
csn-2(ok1288)
csn-6(ok1604)
csn-5(ok1064)
C
wild type
csn-2(ok1288)
csn-6(ok1604)
csn-5(ok1064)
merge
α FBF-1
DAPI
D
wild type
csn-2(ok1288)
csn-6(ok1604)
csn-5(ok1064)
anti-V5::FBF-2
anti-tubulin
E
relative FBF-2 level
1.2
1.0
0.8
0.6
0.4
0.2
0.0
****
****
****
10
6
7
4
N
wild type
csn-2(ok1288)
csn-6(ok1604)
csn-5(ok1064)
F
wild type
csn-2(ok1288)
csn-6(ok1604)
csn-5(ok1064)
merge
αV5::FBF-2
DAPI

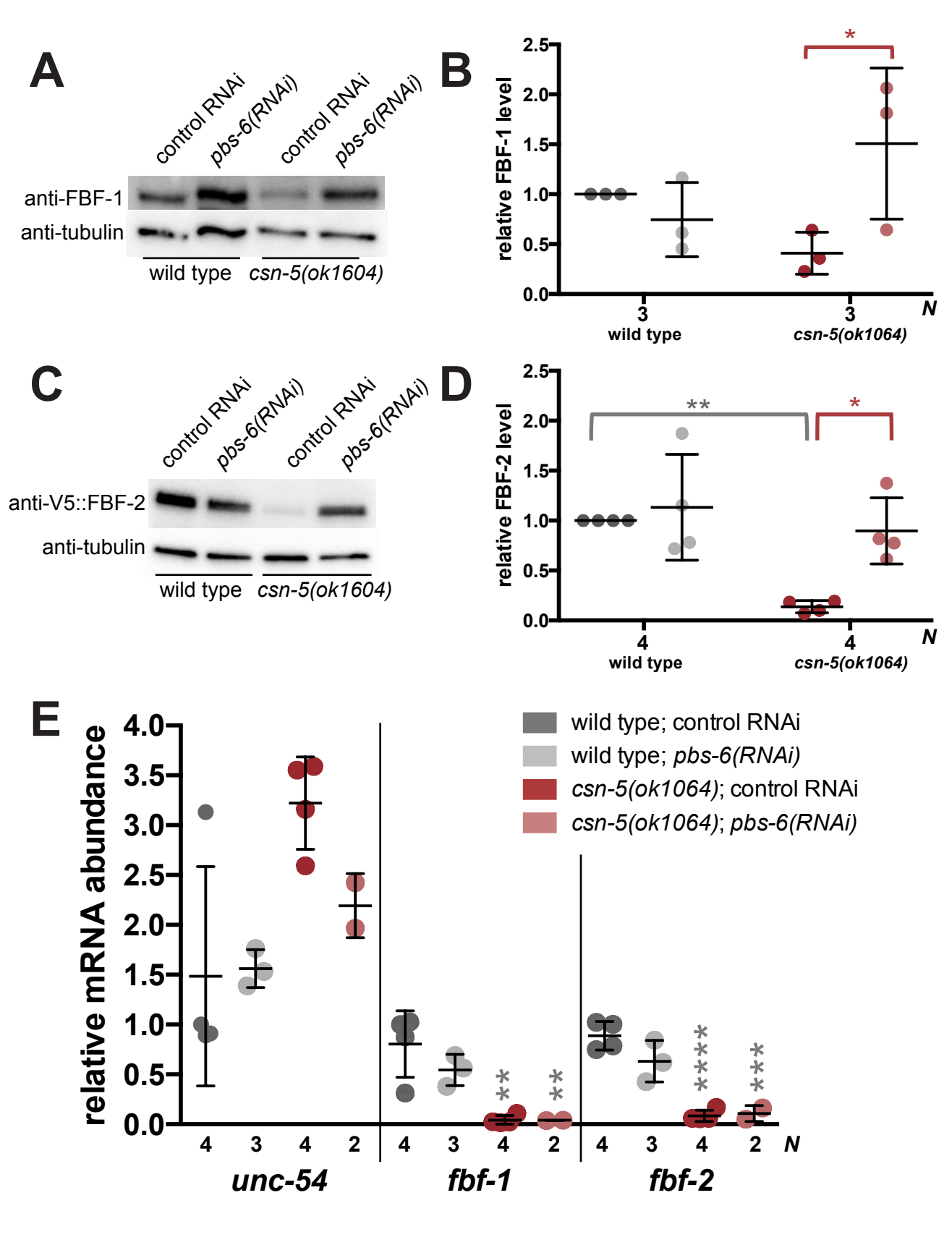
A
control RNAi
pbs-6(RNAi)
control RNAi
pbs-6(RNAi)
anti-FBF-1
anti-tubulin
wild type
csn-5(ok1604)
B
relative FBF-1 level
2.5
2.0
1.5
1.0
0.5
0.0
*
3
3
N
wild type
csn-5(ok1064)
C
control RNAi
pbs-6(RNAi)
control RNAi
pbs-6(RNAi)
anti-V5::FBF-2
anti-tubulin
wild type
csn-5(ok1604)
D
relative FBF-2 level
2.5
2.0
1.5
1.0
0.5
0.0
**
*
4
4
N
wild type
csn-5(ok1064)
E
relative mRNA abundance
4.0
3.5
3.0
2.5
2.0
1.5
1.0
0.5
0.0
wild type; control RNAi
wild type; pbs-6(RNAi)
csn-5(ok1064); control RNAi
csn-5(ok1064); pbs-6(RNAi)
4 3 4 2 4 3 4 2 4 3 4 2 N
unc-54
fbf-1
fbf-2

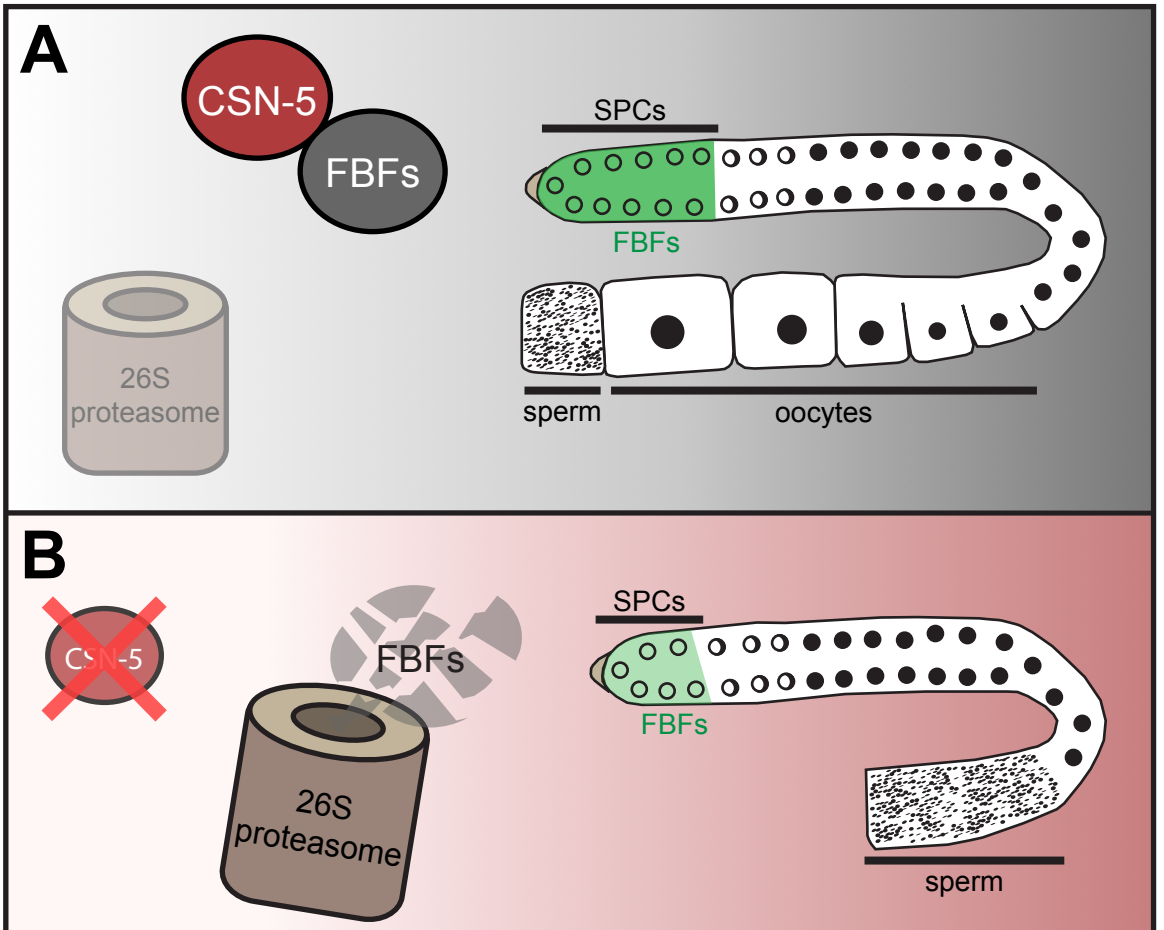
A
CSN-5
FBFs
26S
proteasome
SPCs
FBFs
sperm
oocytes
B
CSN-5
FBFs
26S
proteasome
SPCs
FBFs
sperm